The role of excluded volume effects on the structure and chemical short-range order of $Ni_{33}Y_{67}$ metallic glass

1990 J. Phys.: Condens. Matter 2 8463

(http://iopscience.iop.org/0953-8984/2/42/023)

J. Phys.: Condens. Matter 2 (1990) 8463–8476. Printed in the UK

The role of excluded volume effects on the structure and chemical short-range order of $Ni_{33}Y_{67}$ metallic glass

D Gazzillo†, G Pastore‡ and R Frattini†

† Dipartimento di Chimica Fisica, Università di Venezia, S. Marta 2137, 30123 Venezia, Italy

‡ International School for Advanced Studies, Strada Costiera 11, 34014 Trieste, Italy

Received 19 February 1990, in final form 4 June 1990

Abstract. The possibility of modelling the partial structure factors of the $Ni_{33}Y_{67}$ amorphous alloy with simple purely repulsive potentials is investigated by extending and refining an approach previously proposed for the Ni_xTi_{1-x} alloys. Non-additive hard- and soft-sphere models are carefully studied by using integral equations originally derived in the theory of liquids. The quality of the approximations used and the consequences of softening the repulsion have been examined. The overall agreement between model and experimental data allows a meaningful discussion of the role of different regions of the interaction potential in the real system.

1. Introduction

Accurate determination of the partial structure factors of metallic glasses through the diffraction experiments performed in the last decade has improved our understanding of the structural properties of such systems. The analysis of the experimental data reveals the existence of chemical short-range order (CSRO) effects in many of these materials. In particular, amorphous alloys of late and early transition metals (TM) or late transition and rare-earth metals have shown a considerable degree of compositional order, i.e. a tendency to exhibit microscopic deviations from a random composition to favour hetero-coordination, that is alternation of the two species (see e.g. Fukunaga *et al* (1984), Lee *et al* (1984), Lefebvre *et al* (1985), Wildermuth *et al* (1985), Mizoguchi *et al* (1985), Steeb and Lamparter (1985)). Such a tendency is clearly revealed by examining the experimental Bhatia–Thornton partial structure factors $S_{N-C}(k)$ (Bhatia and Thornton 1970): in fact a strong CSRO produces a sharp peak in the concentration–concentration structure factor ($S_{CC}(k)$) at wavenumbers smaller than the position of the first peak in the number–number structure factor ($S_{NN}(k)$) which describes the 'average' structure, i.e. the topological short-range order (TSRO).

The theoretical interpretation of the microscopic structure of these glasses certainly should be based on a realistic modelling of the interatomic forces. However, our present ability to describe the interactions in *amorphous* TM alloys does not yet allow us to perform accurate and extensive *ab initio* calculations. In addition, it would be highly desirable to get simplified models which could be used for semiquantitative theoretical estimations or for a first analysis of experimental data. For these reasons in a previous paper (Gazzillo *et al* 1989) (hereafter referred to as I) we started an investigation on

0953-8984/90/428463+14$03.50

the applicability of an approach based on liquid theory to model the structure and CSRO in TM amorphous alloys. In I we were able to show that, in the case of the systems Ni_xTi_{1-x}, even at a primitive level where the interaction is mimicked by a hard-sphere repulsion between the ionic cores, a reasonable choice of *three independent* diameters (the *non-additive* hard-sphere model) is able to give good agreement with the experimental data and, in particular, to exhibit CSRO.

In the present paper we use the existing neutron diffraction data on $Ni_{33}Y_{67}$ (Maret *et al* 1985, 1987) to test and extend our previous analysis on a system where the size effects are expected to be more important and CSRO is even higher than in $Ni_{40}Ti_{60}$ (note that in $Ni_{33}Y_{67}$ the ratio of the diameters of the two components, $R_Y/R_{Ni} \approx 1.4$, is larger than in $Ni_{40}Ti_{60}$, $R_{Ti}/R_{Ni} \approx 1.2$, and is actually one of the biggest in binary alloys of TM). In particular here, we extend our previous work by focusing on the following questions:

(i) does a reasonable choice of non-additive diameters of hard spheres exist, that is able to account for most of the experimental diffraction data for the $Ni_{33}Y_{67}$ alloy?

(ii) how reliable are the integral equations of the theory of liquids that we use to describe amorphous states?

(iii) can the residual discrepancies between the hard-sphere model and experiments be reduced by using softer repulsive potentials?

(iv) what can we infer about the real interactions in the system?

In the following sections we shall present the results of our investigations and, we hope, convincing evidence of the usefulness of the non-additive hard-sphere (NAHS) model to interpret the experimental data for these systems. In more detail, the plan of the paper is the following. The next section is dedicated to an analysis of the data for $Ni_{33}Y_{67}$ within the NAHS model presented in I. We test the accuracy of the integral equation approximations used by looking at thermodynamic consistency and comparing the results with those of other approximations. In section 3 we refine the NAHS model by replacing the potential with a softer, purely repulsive, inverse-power law (the non-additive soft-sphere (NASS) model). In section 4, on the grounds of the results of the models, we discuss the role of different ranges of the Ni–Ni effective potential in the determination of the experimental structure. Some final comments and conclusions are collected in the last section.

2. The non-additive hard-sphere model

2.1. The choice of parameters

As discussed in more detail in I, experimental data for binary alloys with strong CSRO indicate that hetero-coordination is accompanied by non-additivity in the excluded volumes, i.e. the closest approach distance between unlike components is smaller than the arithmetic average of the diameters of the pure metals. Therefore, the crudest way to model the effect of the excluded volume in binary mixtures with strong hetero-coordination is through a *non-additive* hard-sphere (NAHS) model, i.e. a two-component system of particles interacting through a pair potential given by

$$u_{ij}(r) = \begin{cases} +\infty & \text{for } r < R_{ij} \\ 0 & \text{for } r \geq R_{ij} \end{cases} \tag{1}$$

where the R_{ij} are the closest approach distances (hard-sphere diameters), with $R_{12} = (R_1 + R_2)(1 + \Delta)/2$ and $\Delta < 0$ (negative non-additivity). The deviations from the value $\Delta = 0$, appropriate for a mixture of 'billiard balls' with two different sizes, correspond to an easier penetration of unlike particles during molecular collisions. This fact, in turn, changes the local compositional order favouring species alternation. The case of positive non-additivity ($\Delta > 0$) is of no concern here since it favours species segregation.

The structural and thermodynamic equilibrium properties of the liquid and amorphous phases of the NAHS model can be evaluated with standard statistical mechanics techniques. In particular the equation of state and the static correlation functions can be evaluated by using general methods of computer simulation (Monte Carlo or molecular dynamics) (Hansen and McDonald 1986). For the liquid phase of NAHS with negative non-additivity a few simulation studies are available (Adams and McDonald 1975, Ballone *et al* 1986, Gazzillo and Pastore 1989). In a dense or amorphous phase very long runs are required to get reliable results. Therefore, cheaper but accurate approximations are more suitable for extensive samplings of the parameter space. To this end we have used the integral equation method, routinely used in the theory of liquids (Hansen and McDonald 1986), to evaluate the pair correlation functions.

Most of the existing integral equations can be put in the form of the following coupled set of equations:

$$h_{ij}(r) = c_{ij}(r) + \sum_l \rho_l \int \mathrm{d}\boldsymbol{r}'\, h_{il}(r')c_{lj}(|\boldsymbol{r} - \boldsymbol{r}'|) \tag{2}$$

$$F_{ij}(c_{ij}, h_{ij}, u_{ij}) = 0. \tag{3}$$

Here, $h_{ij}(r) = g_{ij}(r) - 1$, the $g_{ij}(r)$ are the radial distribution functions (RDF) and the ρ_l are the number densities of the two species. Equations (2), the Ornstein–Zernike equations, can be thought of as defining the direct correlation functions $c_{ij}(r)$. The true approximation is actually contained in (3), the closure, i.e. in the approximate relation between correlation functions and pair potentials.

In the case of hard spheres a popular choice for the closure, which gives good results as compared with computer experiments, is the so-called Percus–Yevick (PY) closure (Hansen and McDonald 1986). This is given by

$$c_{ij}(r) = g_{ij}(r)(1 - \mathrm{e}^{\beta u_{ij}(r)}) \tag{4}$$

which, using the hard-sphere potential given in (1), is equivalent to

$$\begin{aligned} g_{ij}(r) &= 0 \qquad \text{for } r < R_{ij} \\ c_{ij}(r) &= 0 \qquad \text{for } r \geq R_{ij}. \end{aligned} \tag{5}$$

Unlike the additive case ($\Delta = 0$) no analytic solution is known for the PY equations in the general NAHS case. Equations (2) and (5) have to be solved numerically but robust and efficient methods are nowadays available for this. We used Gillan's algorithm (Gillan 1979) to solve the equations on an a grid of 512 points with a spacing $\delta r = 0.05$ Å. Convergence was checked by performing few test calculations using 1024 mesh points. In addition to $g_{ij}(r)$ and $c_{ij}(r)$ the partial structure factors $S_{ij}(k)$ and the Bhatia–Thornton structure factors, number–number ($S_{NN}(k)$),

number–concentration ($S_{NC}(k)$) and concentration–concentration ($S_{CC}(k)$), as well as the 'neutron' scattering intensity ($S^n(k)$) and other structural quantities, were evaluated according to the definitions given in I.

As a first step in our modelling of the experimental structure factors we have looked for the best choice of diameters within the PY approximate integral equations. The goal of such a 'trial and error' fitting procedure was to obtain a set of reasonable values for the R_{ij}, able to reproduce well the overall features of the experimental data in k-space. We weighted more the agreement in the region of the first two peaks than at long and short wavelengths.

In fact, the long-wavelength region is strongly influenced by the thermodynamic sum rules at $k = 0$ which connect the numerical values of the $k = 0$ limit of the structure factors to purely thermodynamic quantities. Since the thermodynamics is significantly influenced by the values of the effective potential in the whole range, including the attractive part, we cannot trust the values of the $S_{ij}(k)$ at small wavenumbers. On the contrary the short-wavelength region is mainly affected by the steepness of the potential. In particular the phases should be shifted toward larger wavenumbers and the decaying rate of the asymptotic oscillations of a hard-sphere system should be slower than in the real system. Within these constraints, using the experimental value of the density (5.4 g cm^{-3} or 0.0412 atoms Å^{-3}) and trying to optimize the agreement in all the structure factors evaluated, our best choice of the diameters R_{ij} corresponds to $R_{\mathrm{NiNi}} = 2.8$ Å, $R_{\mathrm{NiY}} = 2.7$ Å, $R_{\mathrm{YY}} = 3.4$ Å. This result should be compared with the positions of the first peaks in the experimental $g_{ij}(r)$: $R_{\mathrm{NiNi}} = 2.48$ Å, $R_{\mathrm{NiY}} = 2.85$ Å, $R_{\mathrm{YY}} = 3.55$ Å. The values of the optimal Ni–Y and Y–Y diameters are smaller than the experimental sizes of the exclusion holes and in agreement with the general expectation that the hard-sphere diameters should be slightly smaller than the positions of the experimental peaks in r-space. This choice is also essential to ensure a reasonable agreement for the heights and the positions of the peaks in the reciprocal space. As already remarked in I, each $S_{ij}(k)$ is mainly affected by changes in the corresponding R_{ij} (for small changes around a given value). In addition, in the present case the $S_{\mathrm{NiNi}}(k)$ is not very sensitive to the exact choice of R_{NiNi}: in fact, a value as low as 2.4 Å even improves the agreement of the $g_{\mathrm{NiNi}}(r)$ or the first peak of $S_{\mathrm{NiNi}}(k)$ with the experiment. Nevertheless, the value of 2.8 Å is better from a global point of view.

A comparison of the model and experimental structure factors ($S_{ij}(k)$, $S_{N-C}(k)$ and $S^n(k)$) is shown in figures 1, 2 and 3, respectively.

The experimental $S_{\mathrm{YY}}(k)$ is the partial structure factor closest to that of a one-component system. This is consistent with the fact that yttrium is the majority species and the largest one. The PY results follow reasonably well the experimental Y–Y and Ni–Y partial structure factors according to the previously mentioned criterion. Actually the first peak of the experimental $S_{\mathrm{YY}}(k)$ appears slightly asymmetric, with a steeper rising part as compared with the NAHS model, but the following peaks are reasonably well in-phase and their heights agree with the experimental data. The agreement is even better for the $S_{\mathrm{NiY}}(k)$. However, the $S_{\mathrm{NiNi}}(k)$ shows the largest discrepancy between theoretical and experimental data. In particular, the second peak of the experimental data, which looks like two close peaks merged into one with a marked shoulder on the right-hand side, seems to separate into two well-defined peaks at about 2.5 and 3.7 Å^{-1} in the solution of the integral equations. $S_{\mathrm{NiNi}}(k)$ shows no significant structure beyond 5 Å^{-1}, consistent with the experimental results.

The Bhatia–Thornton structure factors embody the same information organized

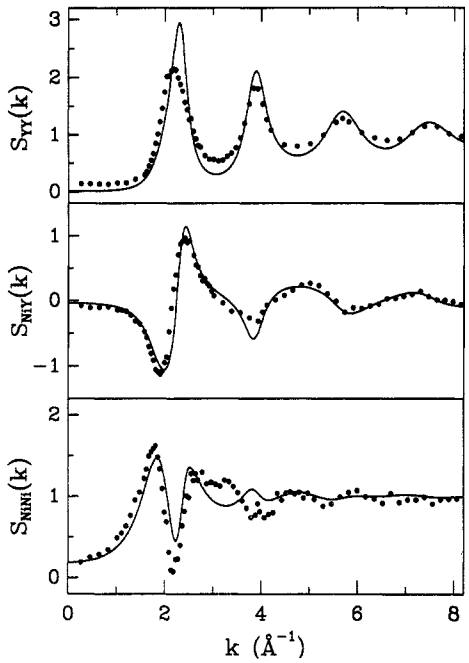

Figure 1. Comparison between the experimental (points) and the PY (full curves) partial structure factors $S_{ij}(k)$.

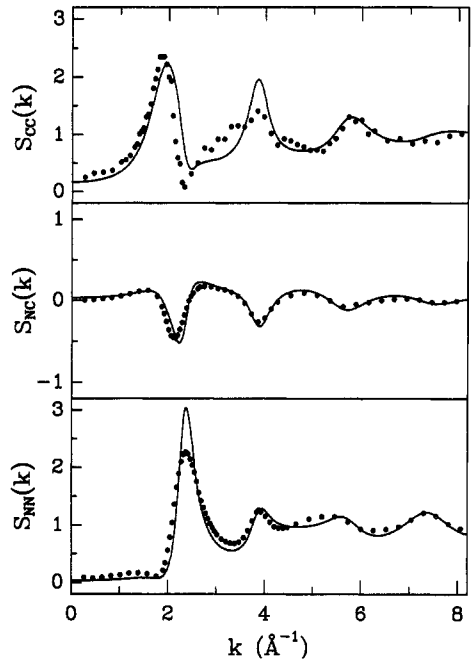

Figure 2. Bhatia–Thornton $S_{N-C}(k)$ structure factors. Labels as in figure 1.

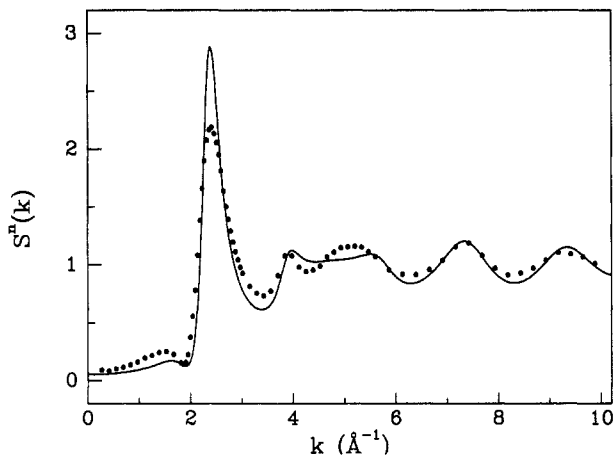

Figure 3. Combination of the partial structure factors corresponding to the neutron scattered intensity $S^n(k)$ from the 'natural composition' sample. Labels as in figure 1.

differently: the non-trivial $S_{CC}(k)$ signals the strong tendency toward compositional order. The discrepancies between theory and experiment, almost completely concentrated in the $S_{\mathrm{NiNi}}(k)$, here are shared by $S_{NN}(k)$ and $S_{CC}(k)$ and are less evident. Due to the neutron scattering lengths of Ni and Y at their natural compositions, $S^n(k)$ closely follows the behaviour of $S_{NN}(k)$. Note, in particular, the second and

the broad third peak of $S_{NN}(k)$ between 3.5 and 6 Å^{-1}. A comparison with the same partial structure factor for $Ni_{40}Ti_{60}$, where the two peaks corresponding to those of $Ni_{33}Y_{67}$ merge into a single broad one, is probably signalling the larger size effect, i.e. the difference in the radii of Ni and Y. The NAHS model is able to reproduce the qualitative features, included this splitting, but the exact position of the third peak as well as its width are not well reproduced.

Also the so-called pre-peak, present in the experimental $S^n(k)$ and $S_{NN}(k)$ at about 1.6 Å^{-1}, appears in the model although slightly underestimated and shifted toward higher wavenumbers.

In conclusion we can say that, taking into account the crudeness of the model, the overall agreement is satisfactory but for the region of the second peak of $S_{\text{NiNi}}(k)$. Small differences in the positions and shapes of the first peaks are visible on a finer scale. The enhanced size and compositional order effects, clearly exhibited by the experimental data for $Ni_{33}Y_{67}$, are quite well reproduced by the model confirming the point of view that not only the TSRO but also the CSRO are mainly determined by excluded volume effects.

The discrepancy in the second peak of $S_{\text{NiNi}}(k)$, like a similar discrepancy in the case of the $Ni_{40}Ti_{60}$ alloy observed in I, calls for a more detailed analysis. In the following we investigate whether it can be accounted for by an improved closure or by continuous repulsive potentials.

2.2. Test of the closure for the NAHS model

The calculation of the static structure using the PY integral equation is not numerically intensive as a computer simulation and avoids all possible problems with non-ergodicity. By construction, the solution of integral equations refers to a hypothetical ergodic homogenous phase. Computer simulations of very closely packed systems usually encounter the problem of being trapped in locked configurations and this phenomenon implies that very long runs are required to lose any dependence on the initial conditions. For these reasons, a check of the integral equation results, which in the liquid phase is usually performed by comparison with computer simulations, appears more delicate in the present case. As an indirect indicator of the quality of the integral equation results we can use a thermodynamic self-consistency criterion, often employed in connection with liquid phase calculations.

One consequence of an approximate closure is the breakdown of some exact sum-rules derivable from a formal treatment of the statistical system, i.e. different routes to the same quantity give different results. Usually, the larger the thermodynamic inconsistency, the worse the comparison of structural results with the 'exact' ones. Although this 'internal' criterion cannot be regarded as very precise, it can be used as a quick measure of the quality of a closure.

We stress that, since we are approximating the structure of a (non-equilibrium) glassy material with that of an *ergodic* supercooled liquid (see I for a more accurate discussion about this point), possible thermodynamic inconsistencies due to the broken ergodicity effects in the real system (Palmer 1982) have no relation with the inconsistencies displayed by approximate liquid state theories. As a matter of fact, these latter inconsistencies are just artifacts, due to the approximations on the exact relation between pair potentials and pair correlation functions and are present even at liquid densities where the real system is ergodic.

One of the simplest inconsistencies to check in an integral equation calculation is that between the isothermal derivative of the virial pressure with respect to the density

and the independent expression for the same quantity (the isothermal bulk modulus) as given by the fluctuation-dissipation theorem. In a two-component homogeneous system one should have the exact equality

$$\left.\frac{\partial \beta P}{\partial \rho}\right|_T = 1 - \rho \sum_{i,j} x_i x_j \hat{c}_{ij}(k=0). \tag{6}$$

Here $\hat{c}_{ij}(k)$ is the Fourier transform of $c_{ij}(r)$, ρ is the total number density, x_i the molar fraction of the species i ($x_i = \rho_i/\rho$) and $\beta = 1/k_B T$, T being the temperature. The virial pressure P is given by

$$\frac{\beta P}{\rho} = 1 + \frac{\rho}{6} \sum_{ij} x_i x_j \int \mathrm{d}r\, g_{ij}(r) \frac{\mathrm{d}\beta u_{ij}}{\mathrm{d}r}(r). \tag{7}$$

In the case of the PY approximation for the NAHS mixtures, with the above mentioned choices of diameters, the discrepancy between the two sides of equation (6) is given in table 1.

Table 1. Bulk moduli obtained from the left-hand (virial) and right-hand (fluctuation) sides of equation (6) with different models and closures.

Model–closure	Virial	Fluctuation
NAHS–PY	124.7	242.7
NAHS–MS	200.0	171.2
NAHS–BPGG	187.6	185.2
NASS–PY	78.7	294.1
NASS–HNC	284.9	138.1
NASS–RY	213.2	214.1

For comparison, we have also made calculations using the Martynov–Sarkisov (Martynov and Sarkisov 1983) (MS) closure, which has been shown to be an improvement on PY also for additive and non-additive HS mixtures (Ballone *et al* 1986) and an improved version of the MS closure recently proposed by two of us (BPGG) (Ballone *et al* 1986).

The BPGG closure in its more general form is given by

$$g_{ij}(r) = \exp\{-\beta u_{ij}(r) + [1 + s_{ij}(h_{ij}(r) - c_{ij}(r))]^{1/s_{ij}} - 1\} \tag{8}$$

where s_{ij} are adjustable parameters. For $s_{ij} = s = 2$ the BPGG closure reduces to the MS closure, while for $s_{ij} = s = 1$ one recovers the hyper-netted-chain (HNC) (Hansen and McDonald 1986) approximation. In general the s_{ij} can be used as free parameters to impose thermodynamic consistency.

As in Ballone *et al* (1986), we have used a simple one-parameter form ($s_{ij} = s$) but we have found that in the present case $s = \frac{15}{7}$ ensures consistency over the range of diameters explored. Results for the radial distribution functions (RDF) obtained with the BPGG closure are practically indistinguishable from the MS results. On the contrary there is a small but visible difference between BPGG and PY results, mainly affecting the contact values of the $g_{ij}(r)$ and the shapes and values of the first minima. Note that, using the closure (8), the RDF are always positive whereas in some cases

the PY first minima may become negative. In any case, we have found that for hard spheres the improvement in the thermodynamic consistency mainly affects the height of the first peak of the $g_{ij}(r)$ and no difference is visible in the *positions* of the peaks of the $S_{ij}(k)$. In conclusion, we tend to exclude the possibility that the qualitative discrepancies in the Ni–Ni structure factor can be due to inaccuracies of the integral equation approach as reflected in the thermodynamic inconsistency.

3. The non-additive soft-sphere model

The comparison of the results from the NAHS model with the experimental data shows that, if the non-additivity is taken into account, most of the features of the diffraction data can be explained in terms of excluded volume effects, i.e. of the size of the regions where the $g_{ij}(r)$ are practically zero. However, the crude assumption of hard-sphere interaction introduces some unrealistic cusps at the contact of the RDF. It is quite obvious that a smoothing of the repulsion should result in a better agreement with the experiments. Moreover, it is interesting to check whether a smooth potential could reduce in any appreciable way the main discrepancy between theoretical and experimental $S_{\mathrm{NiNi}}(k)$ in the region between 2.5 $\mathrm{\AA}^{-1}$ and 4.5 $\mathrm{\AA}^{-1}$.

To stay at the level of simple model potentials, we have therefore investigated the effects of the non-additive soft-sphere (NASS) potentials

$$u_{ij}(r) = \epsilon\left(\frac{\sigma_{ij}}{r}\right)^n \tag{9}$$

with $\sigma_{12} < (\sigma_{11} + \sigma_{22})/2$, which reduce to hard-sphere potentials for $n = \infty$. To appreciate trends, we have chosen a value of $n = 12$ for all the three interactions, although a more detailed representation of the repulsive part of the interactions would probably require different slopes for the different components. The factor ϵ in equation (9) fixes the energy scale. However, due to the way ϵ and σ_{ij} appear in the potential, only the products $\epsilon\sigma_{ij}^{12}$ have a meaning. In the following we conventionally put $\sigma_{\mathrm{YY}} = R_{\mathrm{YY}} = 3.4$ Å and the fitting procedure gives us $\epsilon, \sigma_{\mathrm{NiNi}}$ and σ_{NiY}. We stress that such a choice is purely conventional and no direct relation exists between σ_{ij} and R_{ij}.

In the case of soft potentials we have done some test calculations using the PY, the HNC (Hansen and McDonald 1986) and the thermodynamically consistent Rogers–Young (RY) closures (Rogers and Young 1984). The RY closure can be written as:

$$g_{ij}(r) = \exp[-\beta u_{ij}(r)]\left(\frac{\exp\{f_{ij}(r)[h_{ij}(r) - c_{ij}(r)]\} - 1}{f_{ij}(r)} + 1\right) \tag{10}$$

where the 'mixing functions' $f_{ij}(r)$ have the form $f_{ij}(r) = 1 - \exp(-\alpha_{ij} r)$, thus interpolating between a PY-like closure at small distances and HNC at large distances. We have used $\alpha_{ij} = \alpha = 0.19$ as final value, checking that the deviations from consistency, in the whole parameter range studied, were smaller than some few per cent.

Also in the case of the NASS model, we have explored a range of values to optimize the agreement with the experimental values. The optimal values of the triples ($\epsilon^* = \beta\epsilon, \sigma_{\mathrm{NiNi}}$ and σ_{NiY}) are (1.436, 2.669 Å, 2.768 Å), (4.797, 2.634 Å, 2.634 Å) and (4.305, 2.634 Å, 2.538 Å) for PY, HNC and RY, respectively. The extent of thermodynamical

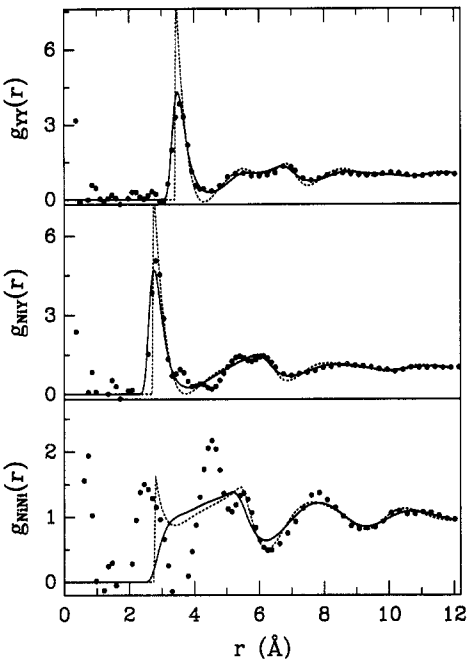

Figure 4. Comparison of the NAHS–PY (dotted curves), NASS–RY (full curves) and experimental (points) radial distribution functions $g_{ij}(r)$.

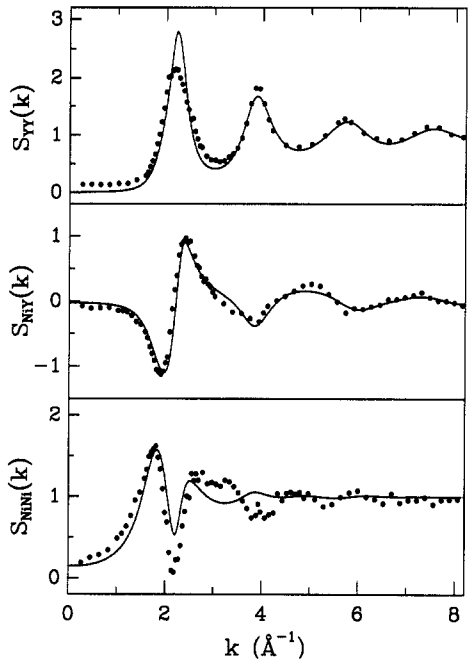

Figure 5. Comparison of the NASS–RY (full curves) and experimental (points) partial structure factors $S_{ij}(k)$.

consistency for these three cases can easily be seen by looking at the second part of table 1.

In figure 4 the RY $g_{ij}(r)$ are compared with both the PY-NAHS results and the relevant experimental functions obtained by Fourier transformation of the $S_{ij}(k)$. As expected, the improvement is in the direction of a more physical shape of the first peak (the oscillations of the experimental data at low r cannot be taken into consideration, since they are spurious and due to noise and truncation of the Fourier transform). The most striking differences occur in the case of $g_{\mathrm{NiNi}}(r)$. Note that, neglecting the unphysical points below 2 Å, the experimental data exhibit a first peak at about 2.45 Å, relevant to Ni–Ni nearest-neighbour contacts, and a second double peak which reveals a preference of the Ni atoms for the second-neighbour shell. As matter of fact, this complex structure is badly reproduced by the NASS and NAHS models. It is worth noting, however, that in some cases, with smaller σ_{NiNi}, the NASS model can also give a smooth first peak separated by the second-neighbour shell. Nevertheless, the reported parameters produce a more satisfactory *global* optimization of r- and k-space results. Furthermore, as we shall discuss more fully in the next section, although in the right direction, a smaller σ_{NiNi} value does not change the structure enough to improve the agreement with $S_{\mathrm{NiNi}}(k)$ significantly.

As shown in figure 5, the overall comparison of the RY $S_{ij}(k)$ with the experiment is similar to that for the NAHS case. The main effect of a softer repulsion is to change the phases of the large-k oscillations and the way the structure factors go to their asymptotic values. On the scale of figure 5 this effect is more evident for the Y–Y component.

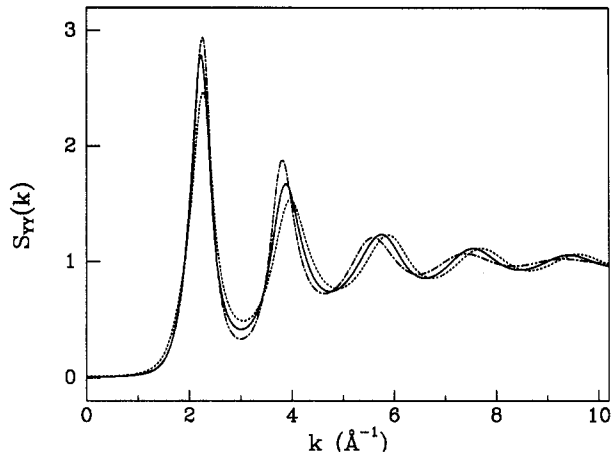

Figure 6. Comparison of the effect of different closures on the NASS $S_{YY}(k)$ partial structure factor: full curve, RY; dotted curve, PY; chain curve, HNC.

At this point some comments are needed to compare the previous RY results with those obtained using the PY and HNC closures (corresponding to $\alpha = 0$ and $\alpha = \infty$, respectively). Varying α from the HNC to the PY value, at fixed σ and ϵ^*, the mean force potential becomes 'harder'. This means a higher structuring of the PY $g_{ij}(r)$ and $S_{ij}(k)$ for a given coupling and it implies the necessity of decreasing the value of ϵ^* in going from PY to HNC to get comparable peak-heights. In addition, in r-space, the smaller α, the larger and steeper the exclusion hole. As a consequence, in k-space one obtains a progressive shift of the oscillations toward larger wavenumbers. The RY case is always in between. To illustrate these considerations, in figure 6 we have plotted the $S_{YY}(k)$ obtained with the three closures.

4. Discussion

As we have discussed in the previous sections, we can attribute most features of the experimental partial structure factors of the $Ni_{33}Y_{67}$ amorphous alloy to the non-additivity of the diameters measuring the size of the exclusion holes of the pair distribution functions. Of course the agreement with the experiment is not complete due to the crudeness of the model. However, the results we have obtained can be used as a first approximation and they allow us to discuss the residual discrepancies, at least on a qualitative basis.

As noted in the previous sections, the main discrepancy between simple repulsive models and experiment is in the region of the second peak of the $S_{NiNi}(k)$. In particular we were not able to reproduce the splitting of the second peak into a double structure with any reasonable value of the 'diameters'. It is possible to interpret such a splitting as the effect of a kind of 'interference' between two characteristic wavenumbers originating from two different lengths in r-space. The presence of a sharply defined shell of first neighbours in the experimental $g_{NiNi}(r)$, followed by a dominant second shell, suggests that the above mentioned lengths could be just related to the positions of these shells. To check this point we have solved the PY equations for the NAHS model at the unphysical value of $R_{NiNi} = 4.0$ Å (corresponding to the position of the rising part of the second peak). Due to the very high resulting coupling the overall

agreement of the structure with the experimental data is poor, but we find that the second-peak position of the theoretical $S_{NiNi}(k)$ now corresponds to the second sub-peak of the experimental second peak instead of being located under the first sub-peak as in all the previous cases.

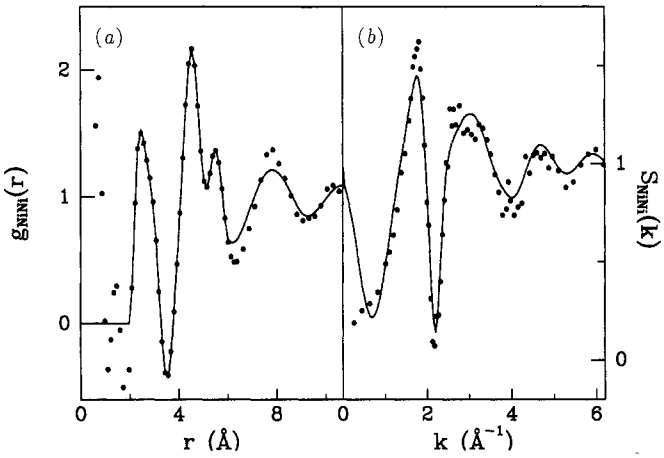

Figure 7. Effect on the $S_{NiNi}(k)$ (b) of including in the NASS–RY $g_{NiNi}(r)$ the experimental shape of the first two peaks (a). Points refer to the experimental data, full curves are the input (a) and output (b) of a numerical Fourier transform.

Furthermore, as a more direct check, we have built an interpolation between the experimental and the NASS–RY $g_{NiNi}(r)$ by joining the theoretical behaviour below 2 Å and above 5.9 Å to the experimental $g_{NiNi}(r)$ in the region of the first two peaks. The result is shown in figure 7. The full curve in part (a) of the figure represents our interpolation as compared with the experimental $g_{NiNi}(r)$ (points). In part (b) the resulting $S_{NiNi}(k)$ are compared. Apart from the spurious behaviour at small wavenumbers, due to the crude matching procedure, we see that now the second peak of the numerical $S_{NiNi}(k)$ is a much better fit to the width of the experimental points although no resolution of separate subpeaks is evident. We consider this result as a confirmation that the structure of the first two shells of neighbours in $g_{NiNi}(r)$ is at the origin of the features of the second peak in the $S_{NiNi}(k)$.

Therefore, since such an effect is related to the interaction with *non-nearest* neighbours, it cannot be explained by *simple* repulsive potentials. On the contrary, it points to a characteristic shape of the *effective* Ni–Ni pair potential in the alloys that could be probably mimicked by a harsh repulsion followed by a repulsive mound.

Due to the averaging implicit in the reduction to pairwise correlation functions, our results cannot be compared directly with possible microscopic models of the local order in $Ni_{33}Y_{67}$. In particular, we are not able to check directly the picture discussed in Maret *et al* (1985) and in Dubois (1985) that tries to relate the diffraction data to a possible superposition, in the amorphous sample, of crystalline structures related to a packing of trigonal prisms observed in Y_3Ni and in Y_3Ni_2 crystalline phases. Indirect information can be obtained from integrated quantities like the coordination numbers.

In table 2 we compare the theoretical coordination numbers, defined as suitable integrals of each partial RDF *up to its first minimum*, to those obtained *with the same definition* from the experimental RDF (note that the definition used in Maret

Table 2. Coordination numbers z_{ij}. They have been omitted whenever the first shell of neighbours it is not well defined. For the experimental z_{NiY} the three values corresponding to the first three minima observed in the RDF have been reported (see text).

Model–closure	z_{NiNi}	z_{NiY}	z_{YY}
NAHS–PY	1.4	7.6	10.3
NAHS–MS	1.2	7.4	10.1
NAHS–BPGG	1.1	6.8	9.0
NASS–PY	—	7.9	11.0
NASS–HNC	—	7.9	10.5
NASS–RY	—	7.7	10.9
Experiment	1.3	(6.8,8.8,10.0)	10.5

et al (1987) is different). There is an overall agreement between experimental and theoretical coordination numbers but some comments are in order.

For the NASS model we have not reported the Ni–Ni coordination numbers because, with our choice of σ_{NiNi}, the first peak of $g_{NiNi}(r)$ has a large overlap with the second shell of neighbours.

The Ni–Y coordination number is probably the most critical for assessing the trigonal-prism-packing picture but, just for this component, there is some ambiguity about the position of the first minimum: the inversion of the experimental $S_{NiY}(k)$ shows three minima after the first peak. If they are real features of the Ni–Y RDF there would be a significant discrepancy between experiment and model in a region where the simple repulsive potential cannot reproduce the features of the real interaction. However, a more quantitative check of this point would require more powerful techniques (like computer simulation). In this respect, an alternative and, in some cases, more convenient method can be represented by a suitable adaptation of the existing computer codes to generate dense random packing of hard spheres by including the non-additivity of the excluded volumes. It is interesting to note that some ad hoc prescriptions used in the past in connection with the standard dense random packing models for binary amorphous alloys (Boudreaux and Gregor 1977) can be easily related to an implicit introduction of a NAHS system.

5. Summary

In this paper we have presented an analysis of the neutron scattering data on $Ni_{33}Y_{67}$ metallic glass based on very simple models which only take into account the geometric excluded volume effects, i.e. the repulsive part of the potentials.

At the simplest level, we have used the NAHS model proposed in I for Ni_xTi_{1-x} alloys. The larger size effect of the $Ni_{33}Y_{67}$ system has allowed us to test the model under more severe conditions and it turns out that also in this case reliable results can be obtained by solving integral equations originally derived in the theory of liquids.

Introducing non-additivity allows most of the observed features of *both* the topological *and* the chemical short-range order to be explained at the same level of accuracy at which simpler systems can be approximated by additive hard-sphere mixtures.

Moreover, we have shown that the model can be refined in various ways. On the one hand, problems related to the PY approximation can be easily overcome by

using thermodynamically more consistent closures. On the other hand, substituting the crude hard-sphere approximation with NASS repulsive potentials increases the flexibility of the model (always concentrating on the next-neighbours interactions).

Further refinements of the interactions are clearly possible. At present, we are investigating the possibility of using Lennard-Jones (LJ) potentials to model the structural properties of Ni–Y glasses. In this respect, we arrive to conclusions similar to those of work by Harris and Lewis (1982, 1983), which was one of the earliest attempts to describe short-range order in transition metal glasses. These authors were able to show that LJ interactions, with parameters adjusted so as to reproduce the short-range order of $Cu_{33}Zr_{67}$, give satisfactory agreement with the experimental data when used in numerical studies to generate dense randomly packed structures. Although the approach of the present paper is consistent with their conclusions, nevertheless it is to be noted that we emphasize the dominant role of the (non-additive) repulsive part of the potentials and we introduce simple liquid state theories as useful tools for a first assessment of the parameter values.

We do not claim that the purely repulsive potentials we have used are anything more than a very crude first approximation to the real interaction. However, we believe that the simple non-additive hard-sphere model is a reasonable starting point for structural investigations of disordered systems. The integral equation approach, of course, can give an insight into the microscopic structure only at the level of a pairwise statistical description. However, it is perfectly possible to use these results as a first step toward an atomic-level investigation. In particular we suggest that dense random packing of *non-additive hard spheres* can represent the local environment of amorphous TM alloys better than additive mixtures.

Acknowledgments

We wish to thank Dr Mireille Maret for sending us a tabulation of the neutron diffraction results. Useful discussions with Dr Stefano Enzo and Dr Riccardo Ceccato are also gratefully acknowledged.

References

Adams D J and McDonald I R 1975 *J. Chem. Phys.* **63** 1900
Ballone P, Pastore G, Galli G and Gazzillo D 1986 *Mol. Phys.* **59** 275
Bhatia A B and Thornton D E 1970 *Phys. Rev.* B **2** 3004
Boudreaux D S and Gregor J M 1977 *J. Appl. Phys.* **48** 5057
Dubois J M 1985 *J. Physique Coll.* **46** C8 335
Fukunaga T, Watanabe N and Suzuki K 1984 *J. Non-Cryst. Solids* **61–62** 343
Gazzillo D and Pastore G 1989 *Chem. Phys. Lett.* **159** 388
Gazzillo D, Pastore G and Enzo S 1989 *J. Phys.: Condens. Matter* **1** 3469
Gillan M J 1979 *Mol. Phys.* **38** 1781
Hansen J P and McDonald I R 1986 *Theory of Simple Liquids* (London: Academic)
Harris R and Lewis L J 1982 *Phys. Rev.* B **25** 4997
—— 1983 *J. Phys. F: Met. Phys.* **13** 1359
Lee A, Etherington G and Wagner C N J 1984 *J. Non-Cryst. Solids* **61–62** 349
Lefebvre S, Quivy A, Bigot J, Calvayrac Y and Bellisent R 1985 *J. Phys. F: Met. Phys.* **15** L99
Maret M, Chieux P, Hicter P, Atzmon M and Johnson W L 1985 *Rapidly Quenched Metals* ed S Steeb and H Warlimont (Amsterdam: Elsevier) p 521
—— 1987 *J.Phys. F: Met. Phys.* **17** 315

Martynov G A and Sarkisov G N 1983 *Mol. Phys.* **49** 1495
Mizoguchi T, Yoda S, Akutsu N, Yamada S, Nishioka J, Suemasa T and Watanabe N 1985 *Rapidly Quenched Metals* ed S Steeb and H Warlimont (Amsterdam: Elsevier) p 483
Palmer R G 1982 *Adv. Phys.* **31** 669
Rogers F J and Young D A 1984 *Phys. Rev.* A **30** 999
Steeb S and Lamparter P 1985 *J. Physique Coll.* **46** C8 247
Wildermuth A, Lamparter P and Steeb S 1985 *Z. Naturf.* a **40** 191